Field Measurements on Piled Rafts with Grid-Form Deep Mixing Walls on Soft Ground

Kiyoshi Yamashita[1], Junji Hamada[2] and Takeshi Yamada[2]
[1]*Deputy General Manager, R&D Institute, Takenaka Corporation, Chiba, Japan, E-mail: yamashita.kiyoshi@takenaka.co.jp*
[2]*Chief Researcher, R&D Institute, Takenaka Corporation Chiba, Japan*

ABSTRACT: Piled raft foundations have been used for many buildings including tall buildings in excess of 150 m in height in Japan, since a piled raft was first used to the four-story building in 1987. This paper offers recent two case histories for an advanced type of piled rafts. The piled rafts combined with grid-form deep cement mixing walls were employed for a seven-story building and a twelve-story building to cope with liquefiable loose sand as well as to reduce consolidation settlements of soft cohesive soil below the loose sand. The high-modulus grid-form soil-cement walls confine the liquefiable loose sand so as not to cause excessive shear deformation to the loose sand during earthquakes. To confirm the foundation design, field measurements were performed on the foundation settlements and load sharing between raft and piles from the beginning of construction to 72 and 27 months after the end of construction for the former and the latter buildings.

Keywords: Piled raft, Grid-form deep mixing wall, Soft ground, Field measurements, Settlement, Load sharing

1. INTRODUCTION

In recent years there has been an increasing recognition that the use of piles to reduce raft settlements can lead to considerable economy without compromising the safety and performance of the foundation (Poulos, 2001; Mandolini et al., 2005). Since the mid-1980s, a lot of piled raft foundations have been employed for high-rise buildings in Germany, mainly in Frankfurt and the detailed investigations for the several high-rise buildings were carried out (Katzenbach et al., 2000). In Japan piled raft foundations have been used for many buildings including tall buildings in excess of 150 m in height since a piled raft was first used to the four-story office building in Urawa in 1987 (Yamashita & Kakurai, 1991; Yamashita et al., 2008).

This paper offers recent two case histories of piled rafts in Japan. The piled rafts supporting a seven-story building and a twelve story-building founded on liquefiable loose sand underlain by soft cohesive soil. To cope with the liquefiable sand and also to reduce settlements of the soft cohesive soil below the loose sand, an advanced type of piled rafts, piled rafts combined with grid-form deep cement mixing walls, were employed for the two buildings. To confirm the validity of the foundation design for the two buildings, field measurements were performed on the foundation settlements, axial loads of the piles, contact pressures between raft and soil (also raft and improved soil), pore-water pressures beneath the raft from the beginning of construction to 72 and 27 months after the end of construction for the former and the latter buildings, respectively. Table 1 shows general description of the two buildings and their foundations (Yamashita & Yamada, 2009; Yamashita & Hamada, 2011).

2. GRID-FORM GROUND IMPROVEMENT

Figure 1 shows grid-form deep cement mixing walls constructed by deep mixing method (TOFT method). The high-modulus soil-cement walls confine loose sand so as not to cause excessive shear deformation to the loose sand during earthquakes. The nominal compressive strength of the soil cement is typically 2 N/mm^2.

The TOFT method was developed late in the 1980s and the effectiveness of the method was highlighted during the 1995 Hyogoken-Nambu earthquake. Figure 2 shows a 14-story building constructed on the pier that faces the Port of Kobe. The building was supported on cast-in-place concrete piles surrounded by the deep cement mixing walls. During the 1995 Hyogoken-Nambu earthquake, the quay walls on the west, south and east of the building moved horizontally by 1 m, 2 m and 0.5 to 0.6 m, respectively. Nevertheless, the building survived without damage to its pile foundations (Tokimatsu et al., 1996).

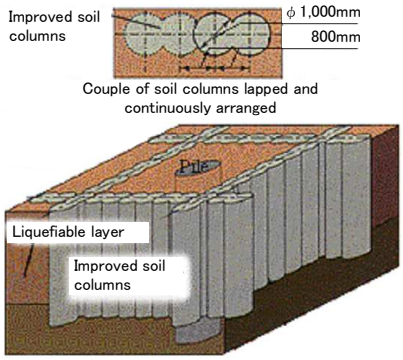

(a) Grid-form soil-cement walls

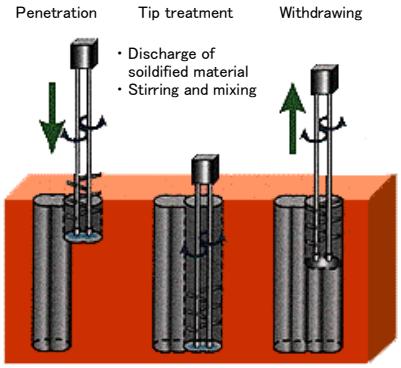

(b) Construction procedure (2-axle type)

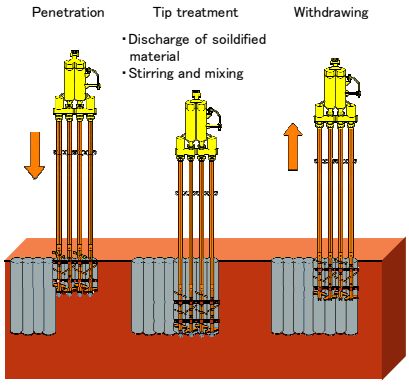

(c) Construction procedure (4-axle type)

Figure 1 Grid-form deep cement mixing walls

3. SEVEN-STORY OFFICE BUILDING

3.1 Building and Soil Conditions

The seven-story office building of 29.4 m in height above the ground surface with a flat dining hall is located in Minamisuna, Tokyo (Photo 1). The building is a steel-frame structure and a schematic view of the building and foundation with soil profile is shown in Fig. 3. The ground water table appears approximately 2 m below the ground surface. The subsoil consists of an alluvial stratum to a depth of 46 m, underlain by a diluvial sandy layer of SPT *N*-values of 50 or higher. The soil profile down to a depth of 11 m is made of soft silt and loose sand. Between depths of 11 m to 42 m below the ground surface, there lies a thick soft to medium silt stratum. The upper silt layer between depths of 11 m to 18 m is slightly overconsolidated with an overconsolidation ratio (OCR) of about 1.1. The lower silt layer between depths of 18 m to 42 m is overconsolidated with an OCR of 1.8 or higher.

3.2 Foundation Design

An assessment of a potential of liquefaction during earthquakes was carried out using the simplified method (Tokimatsu and Yoshimi, 1983). It indicated that the loose sand between depths of 6 m to 11 m had a potential of liquefaction during earthquakes with the peak horizontal ground acceleration of 200 gal. The foundation levels were at depths of 2.2 m in central part and 1.6 m in both ends below the ground surface. Therefore, to cope with the liquefiable sand and ensure bearing capacity of a raft, grid-form deep cement mixing walls were constructed from the foundation level to a depth of 12 m which corresponded to one meter below the bottom of the liquefiable sand (Figs. 1(a) and 1(b)). Photo 2 shows the top surface of the grid-form soil-cement walls (deep cement mixing walls) at the foundation level.

A total load in structural design is 378 MN which corresponds to the sum of dead load and live load of the building. The average contact pressure over the raft is 100 kPa with the local maximum of

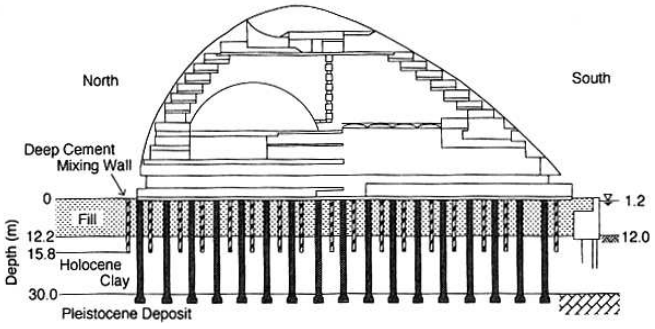

(a) Section

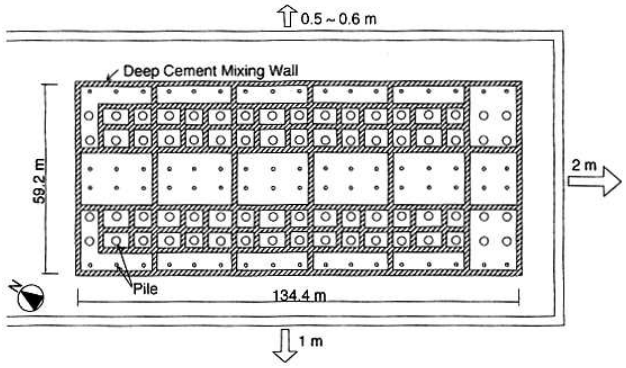

(b) Foundation Plan

Figure 2 Building founded on piles surrounded by Deep Cement Mixing wall (Tokimatsu et al., 1996)

Table 1 General description of structures and foundations

Structure	Site	Construction period	Maximum height (m)	Raft contact pressure (kPa)	Depth of foundation (m)	Depth of groundwater table (m)	Piles			
							Number	Length (m)	Diameter (m)	Pile type
7-story office building	Tokyo	2003-04	29.4	100	1.6, 2.2	1.5	70	29.8, 30.4	0.6-0.9	Bored precast concrete pile
12-story residential building	Tokyo	2007-08	38.7	199	4.8	1.8	16	45.0	0.9-1.2	Bored precast concrete pile

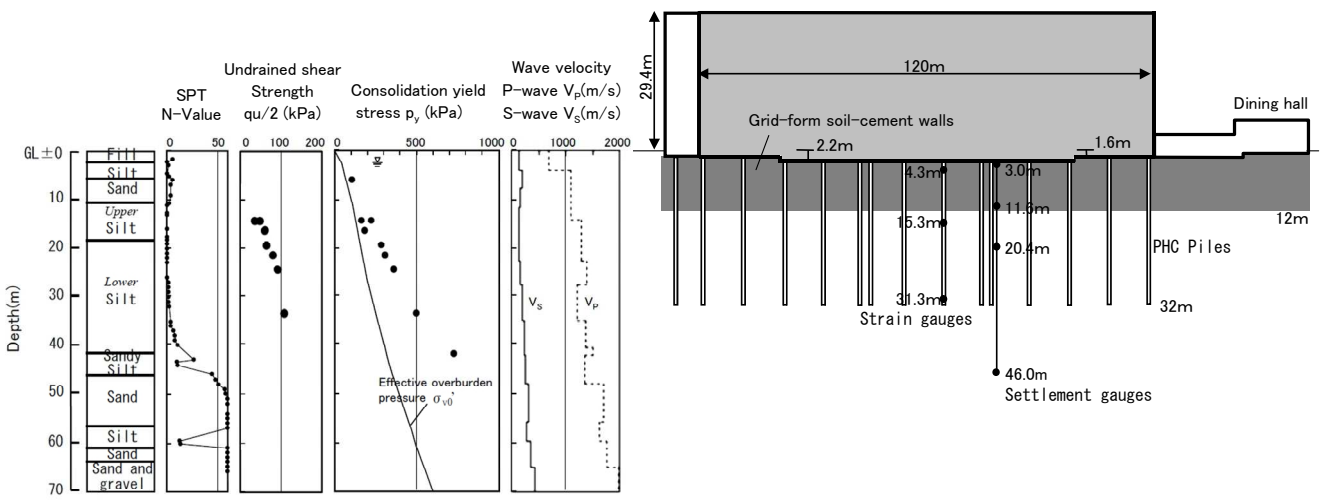

Figure 3 Schematic view of the building and foundation with soil profile

Photo 1 Seven-story office building in Minamisuna

Photo 2 Grid-form soil-cement walls at the foundation level

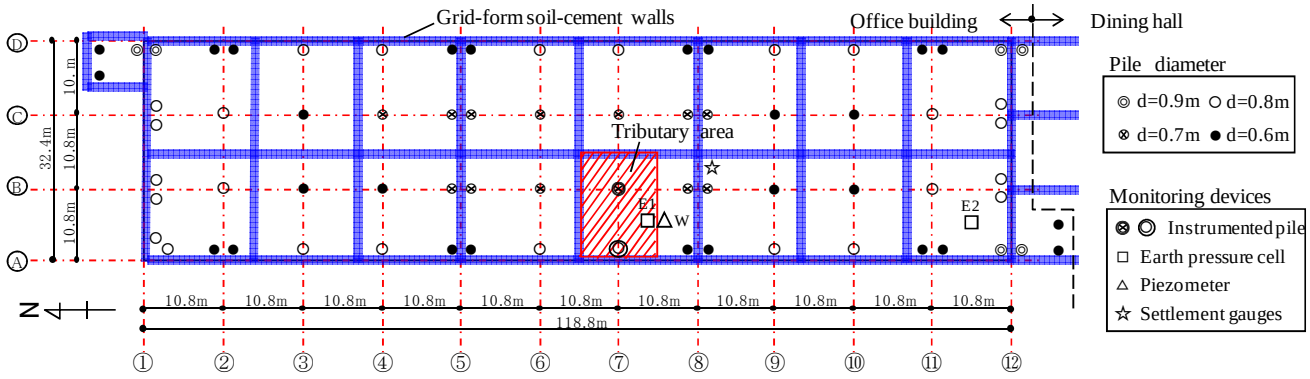

Figure 4 Layout of piles and grid-form soil-cement walls with locations of monitoring devices

142 kPa. If a raft foundation alone was used, more than 200 mm of consolidation settlement was predicted in the soft silt layers down to a depth of 18 m. In order to reduce the consolidation settlement and to ensure the differential settlements being below a tolerable amount, a piled raft was proposed.

The piled raft was designed based on a design philosophy of "creep piling", i.e. sufficient piles are included to reduce the effective contact pressure between raft and soil to below the consolidation yield stress of the clay (Hansbo, 1984; Jendeby, 1986). The allowable bearing capacity of each pile at a working condition was determined to be sufficiently larger than the load which should be carried by the pile based on the "creep piling". At the same time the design load of each pile should be smaller than the load at which significant creep starts to occur, at about 70 % of the ultimate bearing capacity. The piles were embedded in the lower medium silt layer enough to ensure the frictional resistance. Consequently a piled raft supported by seventy 30-m long piles of 0.6 to 0.9 m in diameter with grid-form soil-cement walls was employed.

In the design for vertical loading on the piled raft, numerical analysis was carried out to obtain the foundation settlement and load sharing between raft and piles using the simplified method of analysis developed by Yamashita et al. (1998). The maximum settlement and the maximum angular rotation of the raft were predicted to be 33 mm and 1/1250 radian, respectively, which satisfied the design requirements of 1/1000 radian. The ratio of the load carried by the piles to the total load was set to 0.4 in the design. As for the influence of lateral loading on a piled raft, the bending moment and shear force of the piles were computed using the simplified method proposed by Hamada et al. (2009).

The piles were pretensioned spun high-strength concrete (PHC) piles and were constructed by inserting a set of 15 m-long PHC piles into a pre-augered borehole filled with mixed-in-place soil cement to avoid noise and vibration. Figure 4 shows a layout of the piles and the grid-form soil-cement walls.

3.3 Instrumentation

Field measurements were performed on the foundation settlement, axial loads of the piles and contact pressures between raft and soil as well as pore-water pressure beneath the raft from the beginning of construction to 72 months after the end of construction. The locations of the monitoring devices are shown in Fig. 4. Two piles, 7A and 7B, were installed with a couple of LVDT-type strain gauges at pile head (at a depth of 4.3m). The pile 7B was installed with the other couples of strain gauges at depths of 15.3 m and 31.3 m. Earth pressure cells were installed at depths of 2.2 m (E1) and 1.6 m (E2) and a piezometer (W) was installed at a depth of 2.2 m beneath the raft. The vertical ground displacements below the raft were measured by differential settlement gauges. The settlements of the foundation were measured by an optical level. The reference point was set to an existing nearby building founded on end-bearing piles. The measurement of the axial forces of the piles, contact pressures between raft and soil and pore-water pressure beneath the raft and the vertical ground displacements started early in December 2003, just before the beginning of reinforcement for the 0.3 m thick foundation slab.

3.4 Results of Measurements

3.4.1 Foundation settlement

The building completed in mid-November 2004 and started in operation late in November. In this paper the measurements in 2nd Dec., 2004 are referred to as those "at the end of construction".

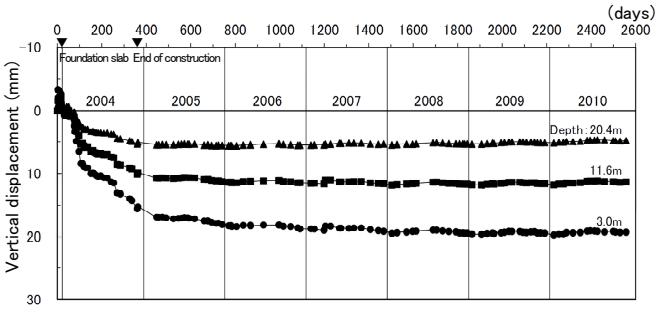

Figure 5 Measured vertical ground displacements

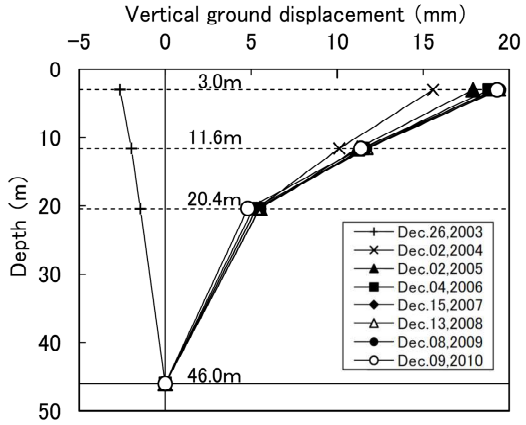

Figure 6 Measured vertical ground displacements with

Figure 5 shows the measured vertical ground displacements below the raft at depths of 3.0 m, 11.6 m and 20.4 m relative to a reference point at a depth of 46 m from the ground surface. The ground displacement at the depth of 3.0 m amounted to 15.6 mm at the end of construction. After that the displacement slightly increased and reached 19.3 mm at 72 months after the end of construction.

Figure 6 shows the distributions of the measured vertical ground displacements with depth. Heaving of the ground due to the excavation amounted to 2.6 mm at a depth of 3.0 m just before casting of the foundation slab (26th Dec., 2003). Including the heaving, the vertical ground displacement at a depth of 3.0 m was 18.2 mm at the end of construction and reached 21.9 mm at 72 months after the end of construction. Figure 7 shows the longitudinal settlement profile of the raft measured by an optical level. The measured settlements were 14 to 24 mm at the end of construction. The settlements slightly increased to 17 to 31 mm at about four years after the end of construction (13th Dec., 2008) and the maximum angular rotation of the raft was 1/1200 radian between the columns 11B and 12B. The measured maximum settlement of the raft and the measured maximum angular rotation were in good agreement with the predicted values.

3.4.2 Pile load and contact pressure

Figure 8 shows the measured axial loads of the piles 7A and 7B. The measured loads at pile head increased after the end of construction, and reached a state of equilibrium for both piles at about four years after the end of construction. Figure 9 shows the distributions of the measured axial loads on the pile 7B. At the end of construction, the average skin friction between depths of 15.3 m to 31.3 m through the layers of soft to medium silt was 90 kPa whereas the value between depths of 4.3 m to 15.3 m through the layers of soft silt and loose sand was 23 kPa. The average skin friction in the lower part of the pile is consistent with the average undrained shear strength of the silt (81 kPa) between depths of 15.3 m to 31.3 m. After that the

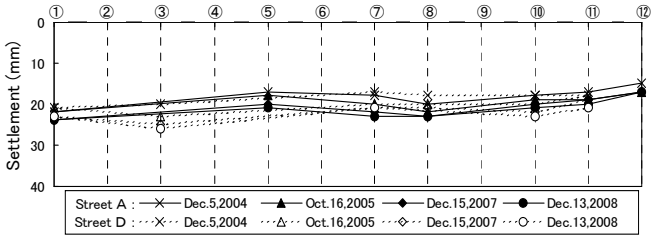

(a) Alignments A and D

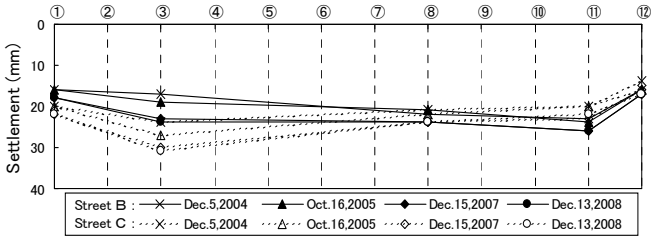

(b) Alignments B and C

Figure 7 Measured longitudinal settlement profiles

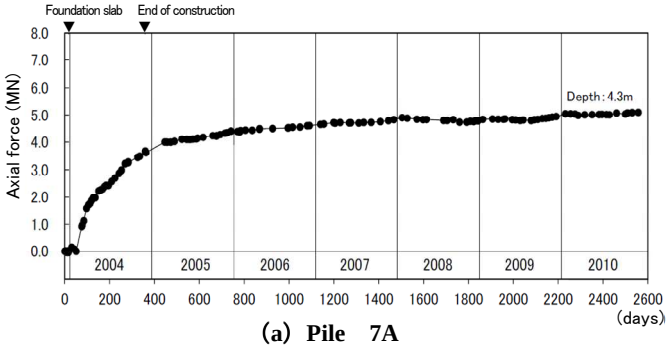

(a) Pile 7A

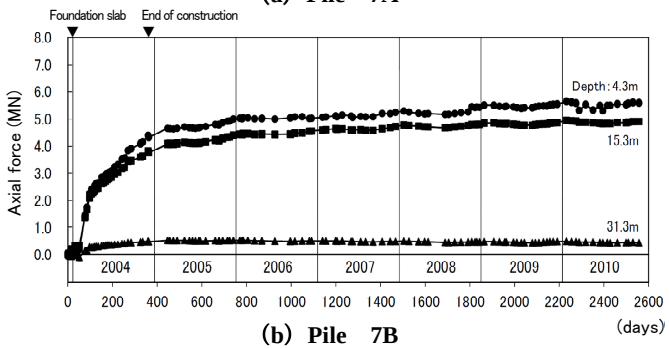

(b) Pile 7B

Figure 8 Measured axial loads of piles 7A and 7B

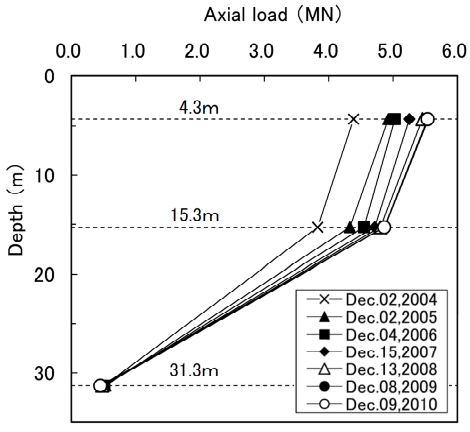

Figure 9 Measured axial load distribution on pile 7B

skin friction in the lower part considerably increased to 127 kPa at 72 months after the end of construction, which is 1.6 times as large as the average undrained shear strength. The skin friction in the upper part slightly increased after the end of construction. Figure 10 shows development of the measured contact pressures of the raft and pore-water pressure beneath the raft. The contact pressures seemed to reach constant values in early stage of construction despite of the successive loading due to construction.

3.4.3 Load sharing between raft and piles

For piled rafts, the equilibrium equation on the tributary area of the columns or piles can be expressed by Eq. (1). Using the measurement results, the ratio of the load carried by piles to the effective load, α_p', the ratio of the load carried by soil to the effective load, α_s', and the ratio of the load carried by improved soil to the effective load, α_g', are given by Eqs. (2), (3) and (4), respectively.

$$W_t' = P_{pt} + (p_{st} - u_{wt})(A_t - A_{pt} - A_{gt}) + (p_{gt} - u_{wt}) A_{gt} \quad (1)$$

$$\alpha_p' = P_{pt} / W_t' \quad (2)$$

$$\alpha_s' = (p_{st} - u_{wt})(A_t - A_{pt} - A_{gt}) / W_t' \quad (3)$$

$$\alpha_g' = (p_{gt} - u_{wt}) A_{gt} / W_t' \quad (4)$$

W_t': effective load (total load minus buoyancy) on the tributary area
P_{pt} : sum of pile-head loads on the tributary area
p_{st} : contact pressure between raft and soil
p_{gt} : contact pressure between raft and improved soil
u_{wt} : pore-water pressure beneath the raft
A_t : plan-view area of the tributary area of the columns or piles
A_{pt} : sum of cross-sectional area of the piles on the tributary area
A_{gt} : plan-view area of improved soil on the tributary area

Figure 11 shows the time-dependent load sharing among the piles, soil, the soil-cement walls and the buoyancy on the tributary area. Assuming that the total load on the tributary area, W_t, given by Eq. (1) is equal to the sum of the design column load on the tributary area, the load sharing between raft and piles can be estimated by Eqs. (2) to (4). Table 2 shows the load-sharing ratios to the effective load on the tributary area at the end of construction and those at 72 months after the end of construction. The ratio of the load carried by the piles to the effective load was estimated to be 0.54 at the end of construction. Thereafter, the ratio of the load carried by the piles gradually increased to 0.72 at the end of observation. On the other hand the ratio of the effective load carried by the grid-form soil-cement walls to the effective load considerably decreased after the end of construction while the ratio of the effective load carried by the soil slightly decreased after the end of construction. As for the raft-soil-pile interaction behaviour on the above, the possible mechanism was as follows:

- Small amount of consolidation settlement occurred in the normally consolidated silt layer below the raft to a depth of 6 m due to loading in excess of the effective overburden pressure of the silt.
- The excessive load transferred to the soil-cement walls and this caused consolidation settlement in the upper silt layer with an OCR of about 1.1 just below the base of the soil-cement walls.
- Consequently a part of the load carried by the soil-cement walls gradually transferred to the piles.

Meanwhile the ratio of the load carried by the piles to the total load was estimated to be 0.50 at the end of construction and 0.66 at the end of observation. The ratio of the load carried by the piles to the total load estimated from the measurements was rather larger than the design assumption. This discrepancy was supposed to be caused by decrease in the raft resistance due to the above-mentioned raft-soil-pile interaction behaviour.

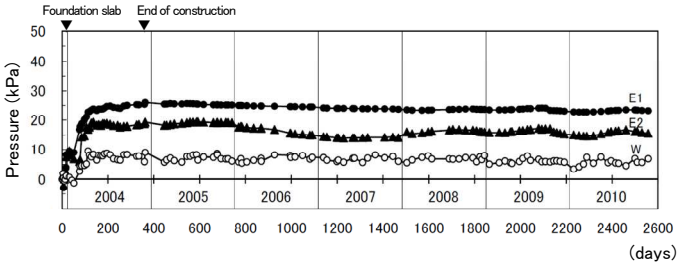

Figure 10 Measured earth pressures and pore-water pressure

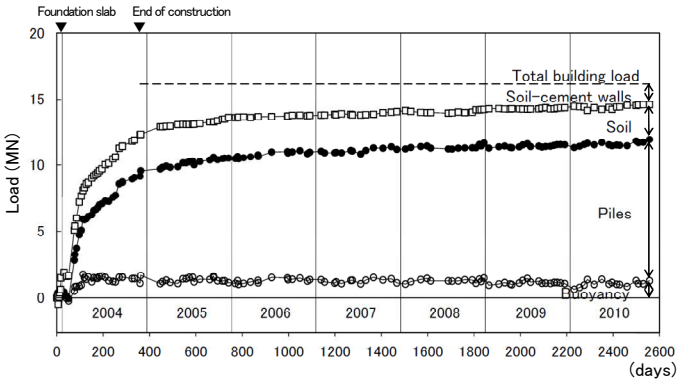

Figure 11 Time-dependent load sharing between raft and piles

Table 2 Load sharing among piles, soil and soil-cement

	At the end of construction	72 months after the end of construction
Ratio of load carried by piles to effective load	0.54 (0.50)	0.72 (0.66)
Ratio of effective load carried by soil to effective load	0.21	0.18
Ratio of effective load carried by soil-cement walls to effective load	0.25	0.10

Values in parentheses indicate ratios of pile load to total load

4. TWELVE-STORY RESIDENTIAL BUILDING

4.1 Building and Soil Conditions

The twelve-story residential building of 38.7 m in height above the ground surface is located in Toyo (Photo 3), at a distance of 0.7 km west from the seven-story building. The building is a reinforced concrete structure with base isolation system of laminated rubber bearings (Photo 4). Figure 12 shows a schematic view of the building and foundation with a typical soil profile. The subsoil consists of an alluvial stratum to a depth of 44 m, underlain by a diluvial sand-and-gravel layer of SPT *N*-values of 60 or higher. The ground water table appears approximately 1.8 m below the ground surface. The soil profile down to a depth of 7 m is made of fill, soft silt and loose silty sand. Between depths of 7 m to 44 m, there lie very-soft to medium silty clay strata. The upper silty clay between depths of 7 m to 15.5 m is slightly overconsolidated with an overconsolidation ratio (OCR) of about 1.5. The lower silty clay between depths of 15.5 m to 44 m is overconsolidated with an OCR of 2.0 or higher.

Photo 3 Twelve-story building in Toyo

Photo 4 Laminated rubber bearings

4.2 Foundation Design

An assessment of a potential of liquefaction during earthquakes was carried and it indicated that the loose silty sand between depths of 3 m to 7 m below the ground surface had a potential of liquefaction. The foundation level was at a depth of 4.8 m, so that the grid-form deep cement mixing walls were introduced to cope with the liquefiable soil below the raft. The grid-form soil-cement walls were constructed using the recently developed 4-axle machine shown in Fig. 1 (c) to reduce the construction period.

A total load in structural design is 198.8 MN which corresponds to the sum of dead load and live load of the building. The average contact pressure over the raft is 199 kPa, twice as much as that for the seven-story building. A bottom depth of the liquefiable sand was at a depth of 7 m. If the grid-form soil-cement walls were constructed to a depth of 7 m or deeper, the bottom of the soil-cement walls would be embedded in the slightly overconsolidated silty clay on which the raft could not have adequate bearing capacity. Therefore, to improve bearing capacity of the raft, the grid-form soil-cement walls were extended to a depth of 16 m with the bottom being embedded in the lower silty clay with undrained shear strength of 75 kPa with OCR of 2 or higher. Furthermore, to reduce settlement and differential settlement to an acceptable level, sixteen 45-m long bored precast piles of 0.9 to 1.2 m in diameter were used. The pile toes were embedded in the very dense sand-and-gravel enough to ensure toe resistance as well as frictional resistance.

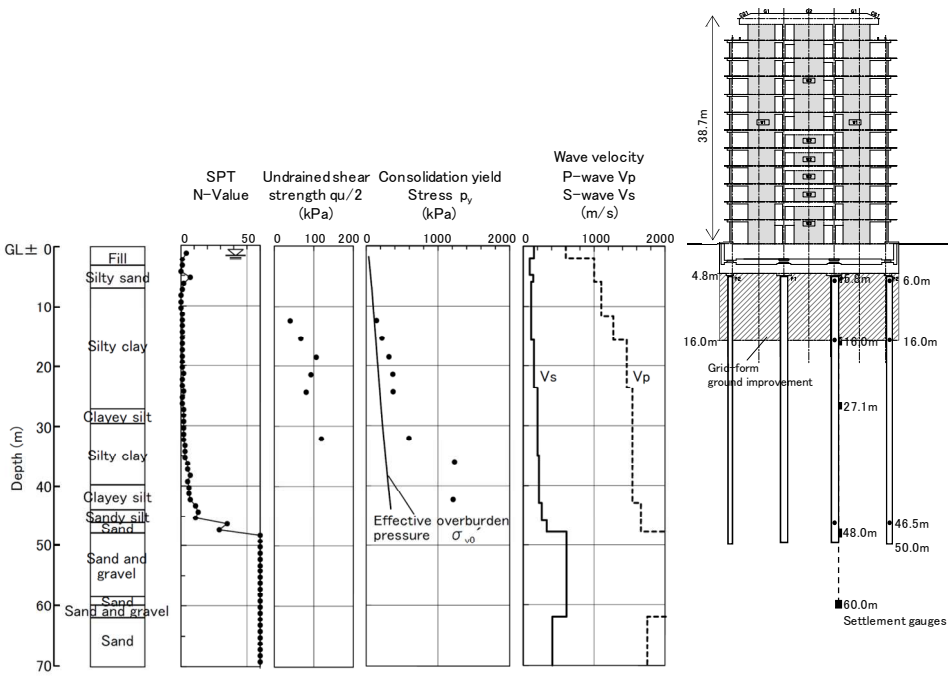

Figure 12 Schematic view of the building and foundation with soil profile

Photo 5 Instrumented PHC piles

Photo 6 Construction of PHC piles (1.2m in diameter)

Numerical analysis was carried out to obtain the foundation settlement and load sharing between raft and piles by means of the simplified method of analysis. The maximum settlement and the maximum angular rotation of the raft were predicted to be 23 mm and 1/1500 radian, respectively, which satisfied the design requirements. The ratio of the load carried by the piles to the total load was set to 0.65 in the design. The pile consisted of a steel pipe-concrete composite (SC) pile used in top portion and PHC piles. Figure 13 shows a layout of the piles and the grid-form soil-cement walls.

4.3 Instrumentation

Field measurements were performed on the foundation settlement, axial loads of the piles and contact pressures between raft and soil as well as pore-water pressure beneath the raft from the beginning of construction to 27 months after the end of construction. The locations of the monitoring devices are shown in Fig. 13. Two piles, 5B and 7B, were provided with a couple of LVDT-type strain gauges at depths of 6.0 m (pile head), 16.0 m and 46.5 m (pile toe) from the ground surface (Photo 5). The pile was constructed by inserting four precast piles (one 12-m long SC pile and two 12-m long and one 9-m long PHC piles) into a pre-augered borehole filled with mixed-in-place soil cement (Photo 6). Near the instrumented piles, eight earth pressure cells and one piezometer were installed beneath the raft at a depth of 4.8 m. The six earth pressure cells E1 to E6 were installed on the intact soil, and the two earth pressure cells D1 to D2 were installed on top of the grid-form soil cement walls. The vertical ground displacements below the raft were measured by differential settlement gauges. LVDT-type transducers were installed beneath the raft at depths of 5.8 m, 16.0 m, 27.1 m and 48.0 m to measure the relative displacements to a reference point at a depth of 60 m as shown in Fig. 12. The settlements of the

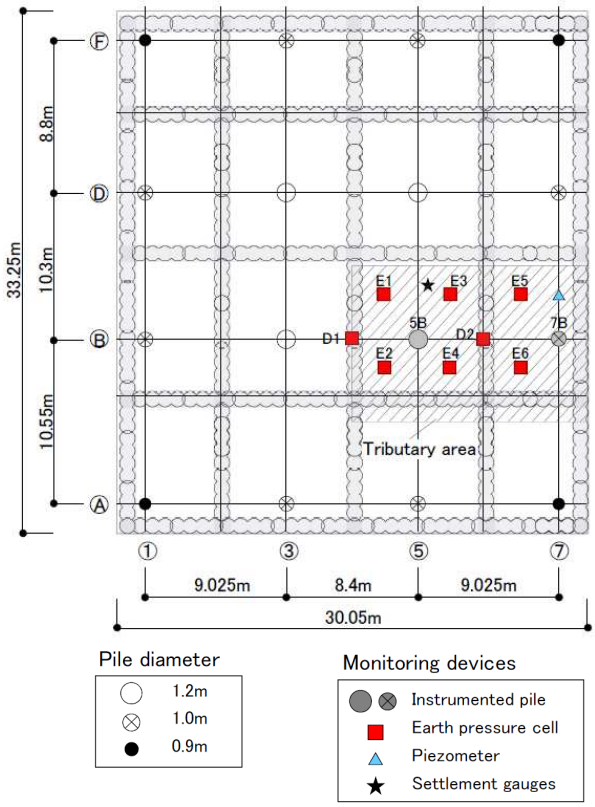

Figure 13 Layout of piles and grid-form soil-cement walls with locations of monitoring devices

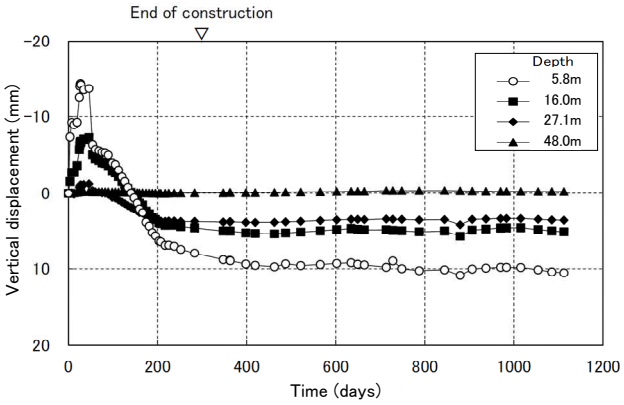

Figure 14 Measured vertical ground displacements

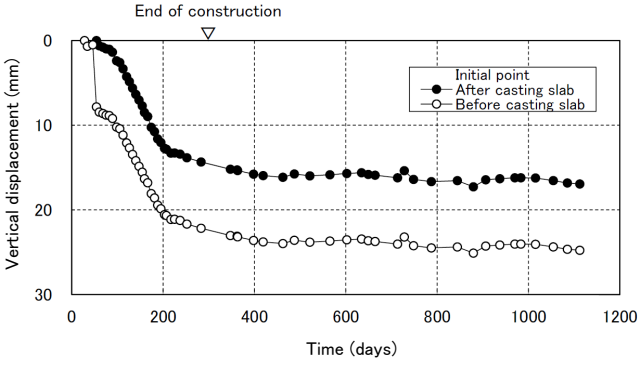

Figure 15 Foundation settlement

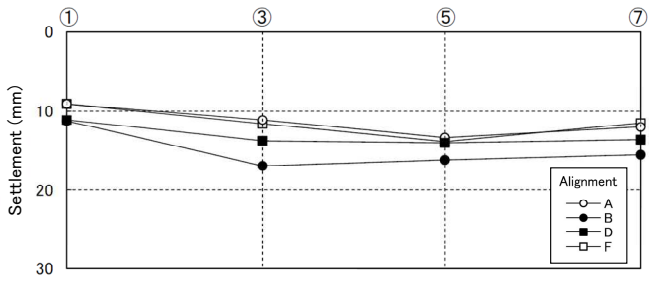

(a) Alignments A, B, D and F

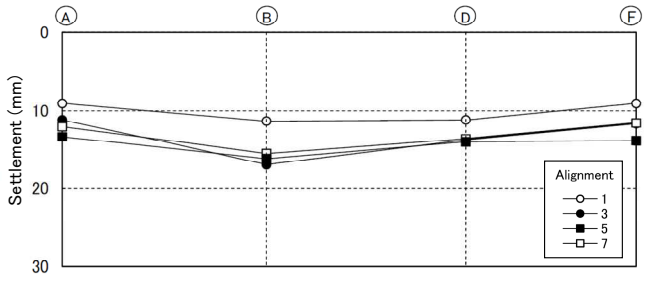

(b) Alignments 1, 3, 5 and 7

Figure 16 Measured settlement profile (at 22 months after E.O.C.)

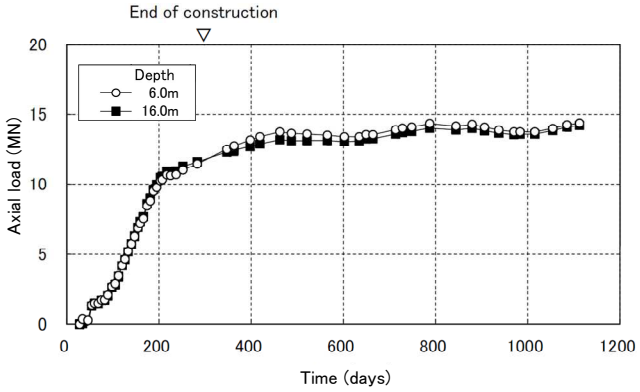

(a) Pile 5B

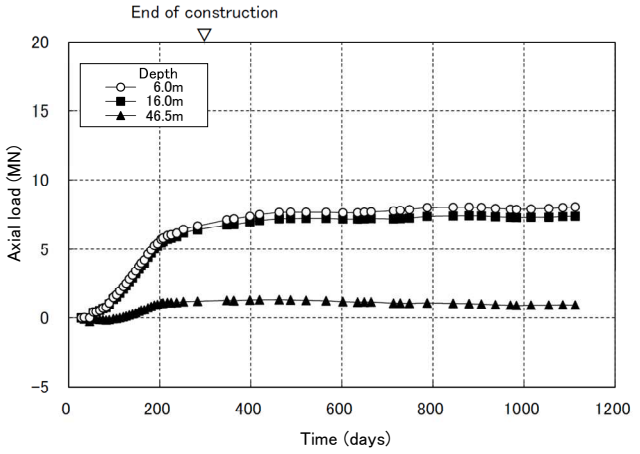

(b) Pile 7B

Figure 17 Measured axial loads of piles 5B and 7B

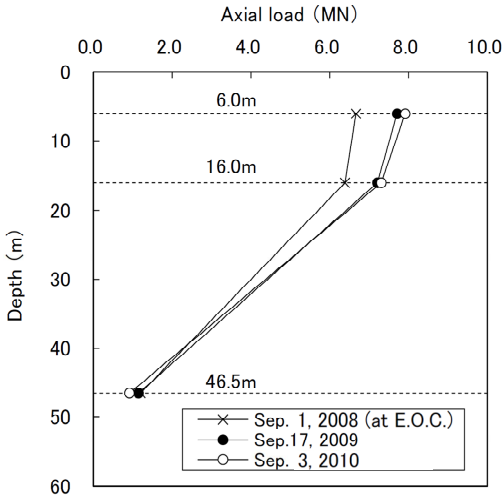

Figure 18 Measured axial load distribution on pile

foundation were measured at the points on the raft by an optical level where the bench mark was set to the monitoring point of the vertical ground displacements.

The measurement of the vertical ground displacements began just before excavation for the foundation construction, late in November 2007. The measurement of the axial loads of the piles, the contact pressures and pore-water pressure beneath the raft began just before the beginning of reinforcement for the 1.5 m thick foundation slab.

4.4 Results of Measurements

4.4.1 Foundation settlement

Figure 14 shows the measured vertical ground displacements below the raft at depths of 5.8 m, 16.0 m, 27.1 m and 48.0 m. At a depth of 5.8 m, the maximum ground heaving due to the excavation was 14.3 mm, and then, immediate settlement of 7.3 mm occurred due to casting of the 1.5 m thick foundation slab. Figure 15 shows the measured ground displacements at a depth of 5.8 m initialised just before the beginning of reinforcement for the foundation slab with those initialised just after the immediate settlement. As the immediate settlement was mostly caused by the self-weight of unset concrete of the raft directly transferred to the soil, the ground displacement initialised just after the immediate settlement is approximately equal to the settlement of 'piled raft'. The settlement of the piled raft reached 14.3 mm at the end of construction and thereafter slightly increased to 16.9 mm at 27 months after the end of construction. Figure 16 shows the settlement profiles of the raft measured by an optical level at 22 months after the end of construction. The measured settlements were 9 to 17 mm and the maximum angular rotation of the raft was 1/1580 radian. The measured maximum angular rotation of the raft was in good agreement with the predicted one while the measured maximum settlement of the raft was slightly less than the predicted one.

4.4.2 Pile load and contact pressure

Figure 17 shows the development of the measured axial loads of the piles 5B and 7B. At the end of construction, the pile-head loads reached 11.5 MN and 6.7 MN on the piles 5B and 7B, respectively. Thereafter, the pile-head loads for both piles slightly increased and reached 14.4 MN and 8.1 MN on the piles 5B and 7B, respectively, at 27 months after the end of construction. Figure 18 shows the distribution of the measured axial loads on the pile 7B. The average skin friction between depths of 6.0 m and 16.0 m was quite small, 9 kPa at the end of construction and 22 kPa at 27 months after the end

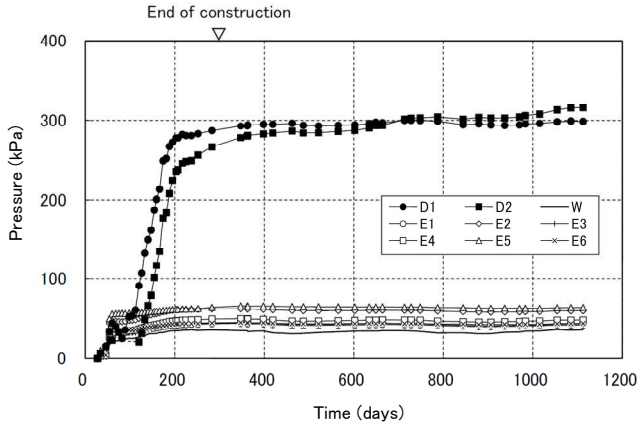

(a) Contact pressures between raft and soil-cement walls and those between raft and soil

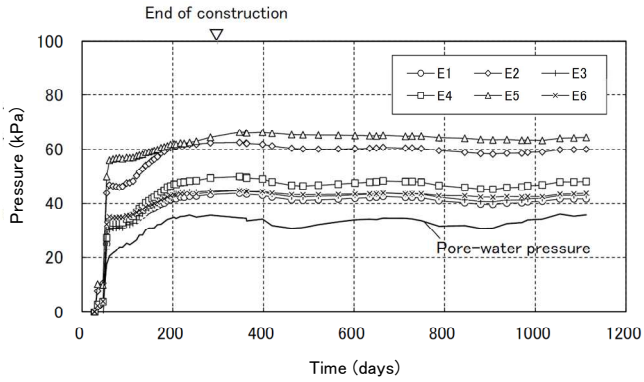

(b) Contact pressures between raft and soil

Figure 19 Measured contact pressures and pore-water pressure

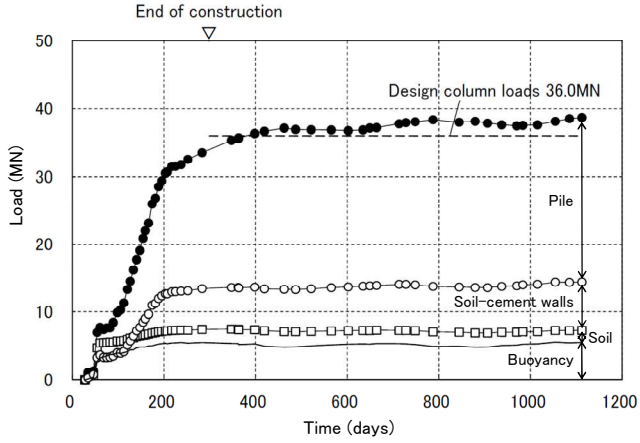

Figure 20 Time-dependent load sharing between raft and piles

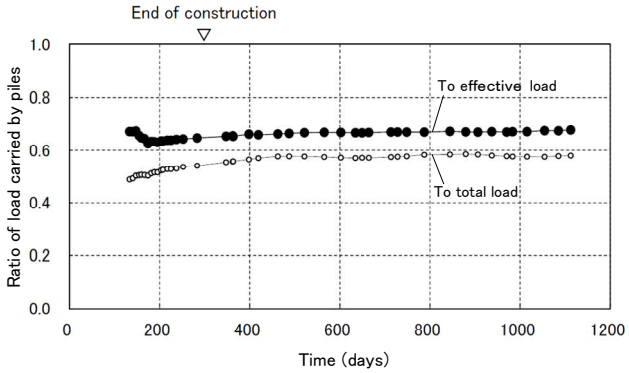

Figure 21 Ratios of load carried by the pile to effective load and total load on the tributary area

Table 3 Load sharing among piles, soil and soil-cement walls

	At the end of construction	27 months after the end of construction
Ratio of load carried by piles to effective load	0.65 (0.54)	0.68 (0.58)
Ratio of effective load carried by soil to effective load	0.07	0.05
Ratio of effective load carried by soil-cement walls to effective load	0.28	0.27

Values in parentheses indicate ratios of pile load to total load

of construction, whereas the average skin friction between depths of 16.0 m and 46.5 m was 54 kPa at the end of construction and 67 kPa at 27 months after the end of construction. The load transferred to the pile toe was relatively small, i.e. the ratio of the pile-toe load to the pile-head load was 0.18 at the end of construction and 0.12 at 27 months after the end of construction. Unfortunately no data were obtained at pile toe of the pile 5B due to disconnection.

Figure 19 shows the development of the measured contact pressures between raft and soil and pore-water pressure beneath the raft. The measured contact pressures between raft and top of the soil-cement walls D1 to D2 increased with construction loading in the same way as the pile-head loads shown in Fig. 17. On the other hand, the measured contact pressures between raft and soil E1 to E6 seemed to reach a state of equilibrium in early stage of construction despite of the successive increase in construction loading. At the end of construction, the measured contact pressures were 266 to 287 kPa from the earth pressures cells D1 and D2, whereas the contact pressures were 43 to 64 kPa from the earth pressure cells E1 to E6. At 27 months after the end of construction, the measured contact pressures between raft and top of the soil-cement walls reached 294 to 304 kPa, which correspond to about six times as large as the measured contact pressures between raft and the intact soil. The contact pressures on the improved soil were quite stable after the end of construction. The measured pore-water pressure was 31 to 35 kPa after the end of construction, which was consistent with the ground water table found by the soil investigation.

4.4.3 Load sharing between raft and piles

Figure 20 shows the time-dependent load sharing among the piles, soil, soil-cement walls and the buoyancy on the tributary area of the columns 5B and 7B shown in Fig. 13. The sum of the measured pile-head loads and raft load on the tributary area after the end of construction was 35.4 to 38.4 MN. The raft load means the load carried by the soil and soil-cement walls and was obtained by use of the contact pressures measured by the earth pressure cells E1 to E6 and D1 to D2. The sum of the measured pile-head loads and raft load on the tributary area is found to be consistent with the sum of the design load of the columns 5B and 7B of 36.0 MN.

Figure 21 shows the ratio of the load carried by the piles to the effective load and that to the total load on the tributary area versus time. Table 3 shows the load sharing between raft and piles. The ratio of the load carried by the piles to the effective load on the tributary area given by Eq. (2) was 0.65 at the end of construction and thereafter slightly increased to 0.68 at 27 months after the end of construction. The ratio of the effective load carried by the grid-form soil-cement walls to the effective load on the tributary area given by Eq. (4) was 0.27 whereas the ratio of the effective load

carried by the intact soil given by Eq. (3) was 0.05 at 27 months after the end of construction. Meanwhile the ratio of the load carried by the piles to the total load on the tributary area was 0.54 at the end of construction and reached 0.58 at 27 months after the end of construction. The ratio of the load carried by the piles to the total load estimated from the measurements was consistent with the design assumption. Based on the measurement results, it was confirmed that the grid-form soil-cement walls carried the raft load successfully.

5. CONCLUSIONS

The advanced type of piled rafts, piled rafts combined with the grid-form soil-cement walls (deep cement mixing walls), were employed for the seven-story building and the twelve-story building to cope with the liquefiable loose sand as well as to reduce consolidation settlements of the soft cohesive soil below the loose sand. To confirm the foundation design, field measurements were performed on the foundation settlements and load sharing between raft and piles from the beginning of construction to 27 to 72 months after the end of construction. Based on the measurement results, the following conclusions are obtained:

- The maximum vertical ground displacements just below the raft, which were approximately equal to the foundation settlements, were 17 to 22 mm at the end of observation. The settlement profiles obtained from the optical level measurements indicated that the maximum foundation settlements and the maximum angular rotation were 31 mm, 1/1200 radian for the seven-story building and 17 mm, 1/1580 radian for the twelve-story building, respectively. The measured maximum settlements and angular rotation of the raft were generally consistent with the predicted values in the design. The ratios of the load carried by the piles to the effective load on the tributary area were estimated to be 0.68 to 0.72 at the end of observation.
- The foundation settlements and the ratios of load carried by piles to effective load were found to be quite stable for a long period after the end of construction. Therefore, it is confirmed that a piled raft combined with grid-form soil-cement walls is effective for the ground consisted of liquefiable loose sand and soft cohesive soil.

ACKNOWLEDGEMENTS

The authors are grateful to Messrs. N. Nakayama, A. Miyashita, H. Abe and Y. Yamaguchi from Takenaka Corporation for their contribution to structural design of the piled rafts. The authors are also grateful to Mr. T. Tanikawa for his efforts in the field measurements.

REFERENCES

HAMADA, J., TSUCHIYA, T. and YAMASHITA, K. (2009). "Theoretical equations to evaluate the stress of piles on piled raft foundation during earthquake", Journal of Structural Construction Eng. (Transactions of AIJ), Vol. 74, No. 644, pp1759-1767 (in Japanese).

HANSBO, S. (1984). "Foudations on friction creep piles in soft clays", International Conference on Case Histories in Geotechnical Engineering, Vol.2, pp914-915.

JENDEBY, L. (1986). "Friction piled foundations in soft clay -A study of load transfer and settlements", Thesis, Chalmers University, Gothenburg, Sweden.

KATZENBACH, R., ARSLAN, U. and MOORMANN, C. (2000). "Piled raft foundation projects in Germany", Design applications of raft foundations, Hemsley J.A. Editor, Thomas Telford, pp323-392.

MANDOLINI, A., RUSSO, G. and VIGGIANI, C. (2005). "Pile foundations: Experimental investigations, analysis and design", *Proc. 16th ICSMGE*, Vol.1, pp177-213.

POULOS, H.G. (2001). "Piled raft foundations: design and applications", *Geotechnique* 51, No.2, pp95-113.

TOKIMATSU, K. and YOSHIMI, Y. (1983). "Empirical correlation of soil liquefaction based on SPT N-value fines content", *Soils & Foundations*, Vol.23, No.4, pp56-74.

TOKIMATSU, K., MIZUNO, H. and KAKURAI, M. (1996). "Building damage associated with geotechnical problems", *Special Issue of Soils & Foundations*, pp219-234.

YAMASHITA, K. and KAKURAI, M. (1991). "Settlement behavior of the raft foundation with friction piles", *Proc. 4th Int. Conf. on Piling and Deep Foundations*, pp461-466.

YAMASHITA, K., YAMADA, T. and KAKURAI, M. (1998). "Simplified method for analyzing piled raft foundations", *Proc. of the 3rd International Geotechnical Seminar on Deep Foundations on Bored and Auger Piles BAP Ⅲ*, pp457-464.

YAMASHITA, K., YAMADA, T. and HAMADA, J. (2008). "Recent case histories on monitoring settlement and load sharing of piled rafts in Japan", *Proc. of the 5th International Geotechnical Seminar on Deep Foundations on Bored and Auger Piles BAP V*, pp181-193.

YAMASHITA, K. and YAMADA, T. (2009). "Settlement and load sharing of a piled raft with ground improvement on soft ground", *Proc. of 17th ICSMFE*, Vol.2, pp1236-1239.

YAMASHITA, K. and HAMADA, J. (2011). "Piled raft with ground improvement for 12-story building on soft ground", *Proc. of 14th ARCSMGE* (to be published).